

Effect of Dose Escalation on the In Vivo Oral Absorption and Disposition of Glycylsarcosine in Wild-Type and *Pept1* Knockout Mice

Dilara Jappar, Yongjun Hu, and David E. Smith

Department of Pharmaceutical Sciences, College of Pharmacy, University of Michigan, Ann Arbor, Michigan

Received June 9, 2011; accepted August 31, 2011

ABSTRACT:

This study evaluated the in vivo absorption and disposition of glycylsarcosine (GlySar), after escalating oral doses, in wild-type and peptide transporter 1 (*Pept1*) knockout mice. [3 H]GlySar was administered to mice at doses of 1, 10, 100, 1000, and 5000 nmol/g b.wt. Serial blood samples were obtained over 480 min, the plasma was harvested, and the area under the plasma concentration-time curve (AUC) was determined. It was observed that the GlySar AUC was 60, 45, and 30% lower in knockout than wild-type mice when evaluated over 2, 4, and 8 h, respectively ($p < 0.01$). Plasma levels of GlySar reached a plateau at 90 min in knockout mice and then rose to a second plateau at 240 min. In wild-type mice, the plasma levels rose continuously to reach a single plateau at 90 min. When

partial AUC (0–120 min) was used as an indicator for rate of absorption, there was a 60% reduction in GlySar absorption rate in knockout mice compared with wild-type animals. Tissue distribution studies were also performed after 10 nmol/g oral doses of [3 H]GlySar. When sampled 1 h after dosing, GlySar tissue concentrations were significantly lower in knockout versus wild-type mice and, with the exception of intestines, reflected differences in the systemic exposure of dipeptide between these two genotypes. Overall, PEPT1 ablation in mice resulted in significant reductions, in vivo, in the rate and extent of GlySar absorption. The AUC of GlySar was proportional to dose in both genotypes over 1 to 100 nmol/g, with minor decrements at the two highest doses.

Introduction

Peptide transporter 1 (PEPT1), a member of the mammalian proton-coupled oligopeptide transporter (POT) family [i.e., PEPT1, PEPT2, peptide histidine transporter-1 (PHT1), and peptide histidine transporter-2 (PHT2)] is an electrogenic symporter that translocates small peptides/mimetics along with protons across a biological membrane via an inwardly directed proton gradient and negative membrane potential (Herrera-Ruiz and Knipp, 2003; Daniel and Kottra, 2004; Brandsch et al., 2008; Rubio-Aliaga and Daniel, 2008). PEPT1 is strongly expressed at the apical membrane of enterocytes in mouse and human small intestine (i.e., duodenum, jejunum, and ileum) with little or no expression in normal colon (Walker et al., 1998; Groneberg et al., 2001; Jappar et al., 2010). However, other POT family members are also expressed in the intestine. For example, transcripts of PHT1 and PHT2 are found in human and rat intestinal tissue segments (Herrera-Ruiz et al., 2001), and immunohistochemical analysis indicates that PHT1 is expressed in the villous epithelium of human small intestine (Bhardwaj et al., 2006). Moreover, PEPT2 is expressed and functionally active in glial cells and tissue-resident macrophages in neuromuscular layers of the gastrointestinal tract (Rühl et al., 2005).

This work was supported by the National Institutes of Health National Institute of General Medical Sciences [Grant R01-GM035498] (to D.E.S.).

Article, publication date, and citation information can be found at <http://dmd.aspetjournals.org>.

doi:10.1124/dmd.111.041087.

PEPT1 is characterized as a high-capacity, low-affinity transporter. It was first cloned from a rabbit intestine cDNA library (Fei et al., 1994), which subsequently led to the cloning of PEPT1 from several mammalian species including human (Liang et al., 1995), rat (Saito et al., 1995), and mouse (Fei et al., 2000). It is highly homologous across species (~80%), contains 12 transmembrane domains with C and N terminals facing the cytosol, and ranges in size from 707 to 710 amino acids, depending on the species (Brandsch et al., 2008; Rubio-Aliaga and Daniel, 2008). Physiologically, intestinal PEPT1 acts to absorb protein digestive products (in the form of di/tripeptides) originating from the diet and gastrointestinal secretions. However, intestinal PEPT1 also acts as a vehicle for the effective absorption of peptide-like drugs with different conformations, sizes, polarities, and charges (e.g., β -lactam antibiotics, angiotensin-converting enzyme inhibitors, renin inhibitors, bestatin, and the antiviral prodrug valacyclovir). Because of its ability to absorb many different therapeutic agents, PEPT1 is viewed as an appealing target in drug development.

PEPT1 may influence drug disposition because of its localization in tissues, which can affect the distribution and/or elimination pathways of peptides/mimetics. For example, PEPT1 is expressed at the apical membrane of S1 segments in kidney proximal convoluted tubules (Shen et al., 1999), thereby having a role in renal reabsorption. PEPT1 is also expressed in pancreas, bile duct, liver, adrenal gland, testes, ovary, and uterus (Fei et al., 1994; Liang et al., 1995; Knutter et al., 2002; Lu and Klaassen, 2006) and, as a result, may have a role in the disposition of small peptide/mimetics in those tissues. PEPT1 is not

ABBREVIATIONS: PEPT1, peptide transporter 1; PHT1, peptide/histidine transporter 1; PHT2, peptide/histidine transporter 2; AUC, area under the plasma concentration-time curve; GlySar, glycylsarcosine; KO, *Pept1* knockout mice; POT, proton-coupled oligopeptide; WT, wild-type mice.

confined to plasma membranes because immunofluorescence microscopy and transport studies have shown this protein to be expressed in lysosomal membranes of liver (Thamotharan et al., 1997), renal (Zhou et al., 2000), and pancreatic cells (Bockman et al., 1997).

Studies in relevant in vivo models of PEPT1 are sparse and confounded, primarily because of the presence of overlapping substrate specificities in animals in which multiple transporters are operative. With the development of *Pept1* null mice (Hu et al., 2008), it is now possible to assess the role, significance, and pharmacokinetic relationships of peptide/mimetic absorption and disposition by PEPT1-mediated mechanisms. Thus, the initial validation studies demonstrated using in vitro (Ma et al., 2011) and in situ (Jappan et al., 2010) methods that PEPT1 accounted for 80 and 95%, respectively, of the total uptake process in jejunum. Likewise, the systemic exposure of GlySar in *Pept1* knockout mice was approximately one-half that of wild-type animals when dosed orally by gavage (Hu et al., 2008). Nevertheless, this latter in vivo study was performed in a limited number of mice ($n = 3-4$) and at only one dose level (i.e., 5 nmol/g b.wt.). In addition, tissue distribution studies were not performed, so the effect of PEPT1 on drug distribution is not known. In the present study, our primary aim is to determine whether PEPT1 exhibits capacity-limited absorption by studying the systemic exposure of a model dipeptide, glycylsarcosine (GlySar), in wild-type and *Pept1* knockout mice during oral dose escalation. Our secondary aim is to characterize the effect of PEPT1 ablation on GlySar tissue distribution.

Materials and Methods

Animals. Wild-type and *Pept1* knockout mice (8–10 weeks old and gender-matched) were used in these experiments (Hu et al., 2008). Mice were housed under temperature-controlled conditions with 12-h light and dark cycles and were provided a standard diet along with water ad libitum (Unit for Laboratory Animal Medicine, University of Michigan, Ann Arbor, MI). Animal studies were performed in accordance with the Guide for the Care and Use of Laboratory Animals as adopted and promulgated by the U.S. National Institutes of Health.

Materials. [^3H]GlySar (14.4 Ci/mmol) and [^{14}C]dextran-carboxyl 70,000 (1.1 mCi/g) were obtained from Moravsek Biochemicals (Brea, CA). Unlabeled GlySar and hydrogen peroxide solution (30%) were supplied by Sigma-Aldrich (St. Louis, MO), and hyamine hydroxide was supplied by MP Biomedicals (Solon, OH). All other chemicals were acquired from standard sources.

Systemic Exposure and Tissue Distribution Studies after Oral GlySar. Wild-type and *Pept1* knockout mice were fasted overnight before each experiment. GlySar was dissolved in normal saline and administered at escalating doses of 1, 10, 100, 1000, and 5000 nmol/g b.wt. [^3H]GlySar (0.5 $\mu\text{Ci/g}$ b.wt.) was added to the aqueous solution and given orally by gavage (20-gauge needle) at a volume of 10 $\mu\text{L/g}$ b.wt. for all doses. Serial blood samples (20 μL) were collected by tail nicks at 0.5, 5, 10, 20, 30, 45, 60, 75, 90, 120, 180, 240, 360, and 480 min. Blood samples were transferred to 0.2-ml thin-walled polymerase chain reaction tubes containing 7.5% potassium EDTA and centrifuged at 3300g for 3 min at ambient temperature. A 5- to 10- μL aliquot of plasma was then transferred to a scintillation vial, and 6 ml CytoScint scintillation fluid (MP Biomedicals) was added to the sample. Radioactivity of the plasma sample was measured on a dual-channel liquid scintillation counter (Beckman LS 6000 SC; Beckman Coulter, Fullerton, CA). It should be noted that mice were returned to their cages between blood sampling where they had free access to water. Food was provided in their cages 4 h after the oral gavage. One and 4 h after oral dosing, mice were given intraperitoneal injections of 0.25 ml warm saline to prevent dehydration. The cage was equipped with a heating pad to help the mice maintain normal body temperature.

After the last blood sample was obtained (8 h), several organs/tissues (e.g., kidney, liver, lung, pancreas, spleen, small and large intestines, bile duct, ovary, testis, prostate, skeletal muscle, heart, eye, and cerebral cortex) were collected. One kidney was collected intact and the other kidney was separated into renal cortex, outer medulla, and inner medulla. The small intestine was cut

into duodenum, proximal jejunum, mid-small intestine, distal ileum, proximal colon, and distal colon; each segment was washed with prewarmed saline solution to remove fecal material and then blotted dry before weighing. Tissue samples were solubilized in 0.5 ml of 1 M hyamine hydroxide for 24 h at 37°C. A 40- μL aliquot of hydrogen peroxide (30%) was then added to each sample and incubated for another 24 h at 37°C. A 6-ml aliquot of CytoScint scintillation fluid (ICN, Irvine, CA) was added to the tissue sample, and radioactivity was measured on a dual-channel liquid scintillation counter.

At 5 min before harvesting the tissues, [^{14}C]dextran (mol. wt. 70,000, 0.15 $\mu\text{Ci/mouse}$) was administered via a tail vein injection to determine the tissue vascular space. As described previously (Ocheltree et al., 2005; Shen et al., 2007), the corrected tissue concentrations of GlySar ($C_{\text{tiss,corr}}$; nmol/g wet tissue) were calculated as follows: $C_{\text{tiss,corr}} = C_{\text{tiss}} - V \times C_{\text{b}}$, where C_{tiss} is the uncorrected tissue concentration of GlySar (nmol/g), V is the dextran space (ml/g), and C_{b} is the GlySar blood concentration (nmol/ml).

A separate tissue distribution study was also performed after a 10 nmol/g oral gavage of [^3H]GlySar. However, in this study organ/tissue and blood samples were collected 1 h after the dose. All other aspects of the experimental design and analysis were similar to that described previously.

Systemic Exposure and Tissue Distribution Studies after Intravenous GlySar. After an overnight fast, wild-type and *Pept1* knockout mice were

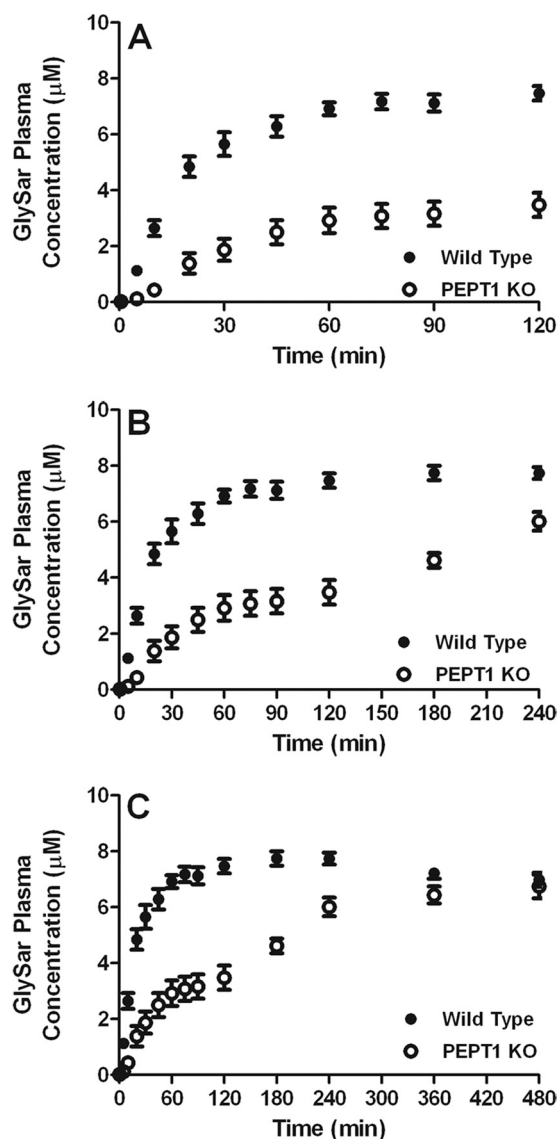


FIG. 1. Plasma concentrations of GlySar as a function of time over 120 (A), 240 (B), and 480 min (C) in wild-type and *Pept1* knockout (KO) mice after an oral gavage of 10 nmol/g. Data are expressed as mean \pm S.E. ($n = 6$).

TABLE 1

Systemic exposure of [³H]GlySar, after escalating oral doses, in wild-type and *Pept1* knockout mice

Data are expressed as mean ± S.E. (n = 4–6).

| Dose (nmol/g) | AUC | | AUC _{KO} /AUC _{WT} | Significance (P) |
|--------------------------|-----------------|-----------------|--------------------------------------|------------------|
| | KO | WT | | |
| <i>min · mM</i> | | | | |
| AUC _{0–120 min} | | | | |
| 1 nmol/g | 0.0276 ± 0.0037 | 0.0673 ± 0.0024 | 0.410 | <0.001 |
| 10 nmol/g | 0.292 ± 0.044 | 0.723 ± 0.034 | 0.404 | <0.001 |
| 100 nmol/g | 3.11 ± 0.35 | 7.14 ± 0.40 | 0.436 | <0.001 |
| 1000 nmol/g | 27.3 ± 6.0 | 61.6 ± 1.4 | 0.443 | <0.001 |
| 5000 nmol/g | 89.8 ± 6.3 | 265 ± 17 | 0.339 | <0.001 |
| AUC _{0–240 min} | | | | |
| 1 nmol/g | 0.0872 ± 0.0098 | 0.153 ± 0.002 | 0.570 | <0.001 |
| 10 nmol/g | 0.854 ± 0.074 | 1.64 ± 0.06 | 0.521 | <0.001 |
| 100 nmol/g | 8.91 ± 0.63 | 15.5 ± 0.9 | 0.575 | <0.001 |
| 1000 nmol/g | 76.0 ± 11.2 | 133 ± 2 | 0.571 | <0.01 |
| 5000 nmol/g | 284 ± 21 | 571 ± 27 | 0.497 | <0.001 |
| AUC _{0–480 min} | | | | |
| 1 nmol/g | 0.234 ± 0.014 | 0.312 ± 0.003 | 0.750 | <0.01 |
| 10 nmol/g | 2.39 ± 0.14 | 3.39 ± 0.10 | 0.705 | <0.001 |
| 100 nmol/g | 23.9 ± 0.8 | 31.6 ± 1.4 | 0.756 | <0.01 |
| 1000 nmol/g | 188 ± 18 | 270 ± 2 | 0.696 | <0.01 |
| 5000 nmol/g | 803 ± 57 | 1128 ± 59 | 0.712 | <0.01 |

KO, *Pept1* knockout mice; WT, wild-type mice.

anesthetized with sodium pentobarbital (40–60 mg/kg i.p.). The mice were then given a 10 nmol/g i.v. bolus dose of [³H]GlySar (0.25 μCi/g) at a volume of 5 μl/g. Serial blood samples were collected by tail nicks at 0.25, 2, 5, 15, 30, 60, 120, 180, 240, 360, and 480 min after the initial dose. Once the last blood sample was obtained (8 h), several organs/tissues were collected, as described previously for oral GlySar dosing. With the exception of mice being anesthetized for 2 h, all other aspects of the experimental design and analysis were similar to that described previously.

Data Analysis. Area under the plasma concentration-time curve (AUC) of GlySar was determined by a noncompartmental approach (WinNonlin version 5.0; Pharsight, Mountain View, CA). Data are reported as mean ± S.E. Statistical differences between wild-type and *Pept1* knockout mice were determined using a two-sample Student’s *t* test. For multiple treatment groups, a one-way analysis of variance was performed followed by Dunnett’s test for pairwise comparisons with the control group (Prism version 4.0; GraphPad Software Inc., La Jolla, CA). *p* ≤ 0.05 was considered statistically significant.

Results

Absorption Profile and Systemic Exposure of GlySar after Escalating Oral Doses. As shown in Fig. 1, wild-type and *Pept1* knockout mice had very different absorption profiles of GlySar, as analyzed over 120, 240, and 480 min, respectively, after the 10 nmol/g dose. In wild-type mice, GlySar plasma concentrations rose rapidly and reached a single plateau level at approximately 90 min. In contrast, GlySar plasma levels in *Pept1* knockout mice reached an initial plateau at approximately 90 min and then rose to a second plateau at approximately 240 min. Moreover, the oral absorption of GlySar was substantially reduced in *Pept1* knockout compared with wild-type mice (*p* < 0.01), as judged by the extent of systemic exposure (AUC), especially during the first 2 h. Similar absorption profiles and AUC differences were observed at the 1, 100, 1000, and 5000 nmol/g doses (data not shown). In fact, when all five doses were considered, the systemic exposure of GlySar in *Pept1* knockout mice was approximately 40, 55, and 70% of that achieved in wild-type animals over the 120-, 240-, and 480-min time periods, respectively (Table 1).

To further illustrate differences in the absorption rate of GlySar between genotypes, partial AUC versus time profiles after the 10-nmol/g dose are shown in Fig. 2. As observed in wild-type mice, the

curve had a single slope from 20 to 480 min. However, for *Pept1* knockout mice, the curve had two distinct slopes from 20 to 480 min; a slower slope from 20 to 120 min and a faster slope from 240 to 480 min, which was parallel to that of wild-type mice. The transition point for the two slopes in *Pept1* knockout mice was approximately 180 min on the basis of our observation of the data and the confines of experimental design. As shown in Table 2, the initial slope (20–120 min) was 60% lower in *Pept1* knockout mice compared with wild-type animals for all five dose levels. In contrast, the latter slope (240–480 min) was very similar between the two genotypes (~10% difference).

To probe whether the PEPT1-mediated absorption of GlySar was capacity-limited, the in vivo systemic exposure of dipeptide was evaluated after escalating oral doses of 1 to 5000 nmol/g in both genotypes. As demonstrated in Fig. 3, the extent of absorption appears linear for wild-type and *Pept1* knockout mice over the 1 to 100 nmol/g dose range because no significant changes were observed in the dose-corrected AUC values of GlySar. Although statistically significant differences were observed at the two highest dose levels, these

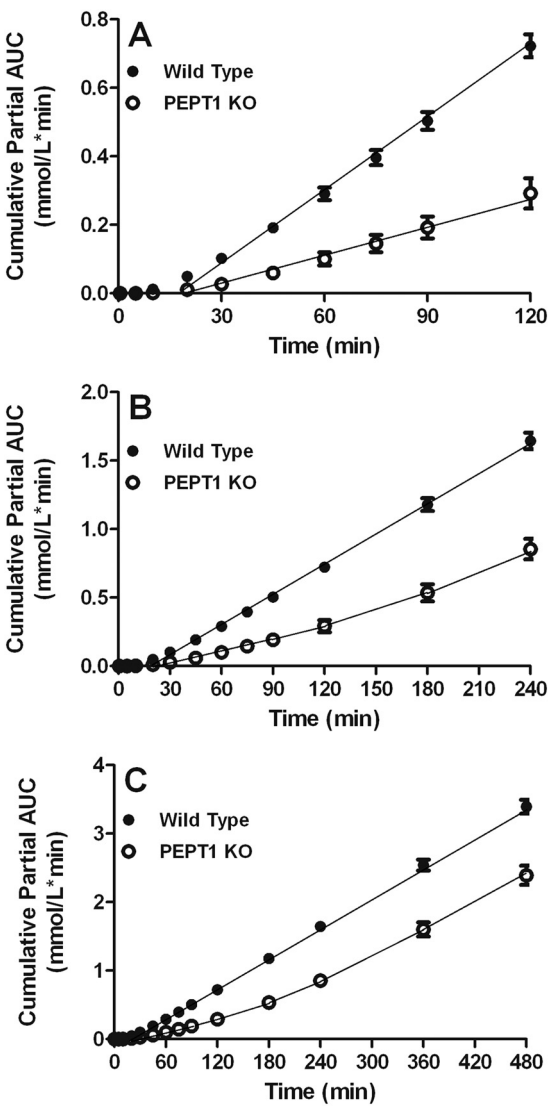


FIG. 2. Partial AUC of GlySar as a function of time over 120 (A), 240 (B), and 480 min (C) in wild-type and KO mice after an oral gavage of 10 nmol/g. Data are expressed as mean ± S.E. (n = 6). The lines highlight linearity and the biphasic nature of GlySar absorption rates.

TABLE 2

Slopes of dose-corrected partial AUC versus time plots of [^3H]GlySar in wild-type and *Pept1* knockout miceData are expressed as mean \pm S.E. ($n = 4-6$).

| Dose | Analyzed from 20–120 min | | | Analyzed from 240–480 min | | |
|-------------|--------------------------|-----------------|-------|---------------------------|-----------------|-------|
| | KO | WT | KO/WT | KO | WT | KO/WT |
| 1 nmol/g | 0.27 \pm 0.02 | 0.64 \pm 0.02 | 0.42 | 0.61 \pm 0.07 | 0.66 \pm 0.01 | 0.93 |
| 10 nmol/g | 0.28 \pm 0.03 | 0.68 \pm 0.02 | 0.42 | 0.64 \pm 0.06 | 0.73 \pm 0.05 | 0.88 |
| 100 nmol/g | 0.30 \pm 0.02 | 0.67 \pm 0.02 | 0.45 | 0.62 \pm 0.04 | 0.67 \pm 0.07 | 0.94 |
| 1000 nmol/g | 0.27 \pm 0.04 | 0.56 \pm 0.02 | 0.48 | 0.47 \pm 0.08 | 0.57 \pm 0.01 | 0.82 |
| 5000 nmol/g | 0.17 \pm 0.01 | 0.49 \pm 0.02 | 0.36 | 0.43 \pm 0.05 | 0.46 \pm 0.05 | 0.93 |

KO, *Pept1* knockout mice; WT, wild-type mice.

changes were small (i.e., <20 and 35% reduction, respectively, at 1000 and 5000 nmol/g) and in the same direction for both genotypes.

Systemic Exposure of GlySar after an Intravenous Bolus Dose.

Fig. 4 depicts the plasma concentration-time profiles of GlySar in wild-type and *Pept1* knockout mice after a 10 nmol/g i.v. bolus dose. As observed in both genotypes, there is a rapid initial decline in

plasma concentrations over the first 1 h followed by a protracted terminal disposition phase over the next 7 h. As a result, it was not possible to obtain an accurate assessment of the terminal half-life of GlySar and its extrapolated area for $\text{AUC}_{(0-\infty)}$ determinations. Still, as evaluated over 8 h, there was a small but significant 24% difference in $\text{AUC}_{(0-480 \text{ min})}$ between wild-type and *Pept1* knockout mice ($p < 0.05$).

Tissue Distribution of GlySar after Oral and Intravenous Dosing. To capture the tissue distribution of GlySar during its initial absorptive phase, experiments were performed 1 h after dosing the dipeptide orally at 10 nmol/g. As shown in Fig. 5A, PEPT1 ablation had a major impact on the accumulation of GlySar in almost all tissues studied. In particular, GlySar accumulation was approximately 7-fold lower in the duodenum of *Pept1* knockout mice than that in wild-type animals. The accumulation of GlySar in all other tissues was 2- to 4-fold lower in mice lacking PEPT1. Because systemic plasma concentrations were the driving force for GlySar distribution in all tissues except the intestines and were dramatically different between the two genotypes 1 h after oral dosing (Fig. 1), the data were also expressed as tissue-to-plasma ratios (except for intestines) to rule out any differences being due to systemic exposure alone. As shown in Fig. 5B, no statistical differences were observed in the tissue-to-plasma concentration ratios of GlySar in wild-type and *Pept1* knockout mice in these nonintestinal tissues.

To capture the tissue distribution of GlySar during its late absorptive and disposition phases, experiments were performed 8 h after dosing the dipeptide orally and intravenously at 10 nmol/g. When administered orally, GlySar accumulation was almost 10-fold lower in the duodenum ($p < 0.001$) and 1.5-fold lower in the distal ileum ($p < 0.05$) of *Pept1* knockout mice compared with wild-type animals (Fig. 6A); no statistical differences were observed in any other tissues between the two genotypes. Likewise, no differences were observed between wild-type and *Pept1* knockout mice when the tissue concentrations of GlySar (intestines omitted) were normalized by their corresponding plasma concentrations (Fig. 6B). When administered intravenously, GlySar accumulation was 1.5- to 9.5-fold lower in several tissues (i.e., testis, pancreas, heart, small and large intestines, skeletal muscle, eye, and cerebral cortex) of *Pept1* knockout mice than that in wild-type animals (Fig. 7A). However, when the tissues were normalized for differences in plasma concentration (including the intestines), these statistical differences disappeared, except for that in mid-small intestine ($p < 0.05$; Fig. 7B).

Discussion

In this study, we report several new findings regarding the in vivo oral absorption and disposition of GlySar in wild-type and *Pept1* knockout mice. In particular, we found the following: 1) PEPT1 ablation caused significant reductions in the systemic exposure of GlySar after oral doses of 1–5000 nmol/g; 2) the oral absorption

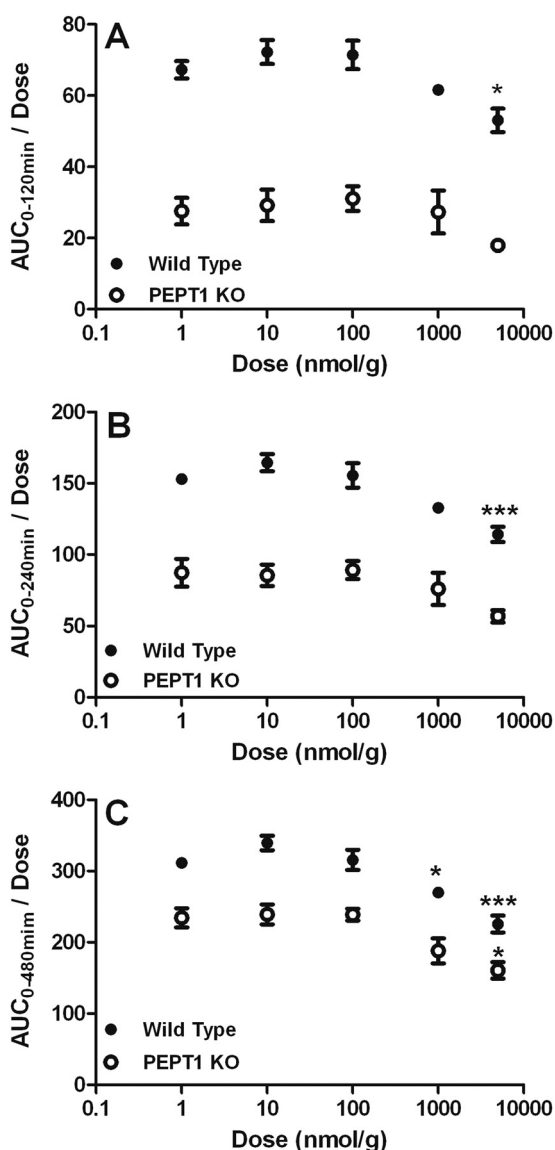


FIG. 3. Dose-corrected area under the plasma concentration-time curves (AUC/Dose) as a function of oral dose over 120 (A), 240 (B), and 480 min (C) in wild-type and KO mice. Data are expressed as mean \pm S.E. ($n = 4-6$). *, $p < 0.05$; and ***, $p < 0.001$ compared with the 1 nmol/g dose.

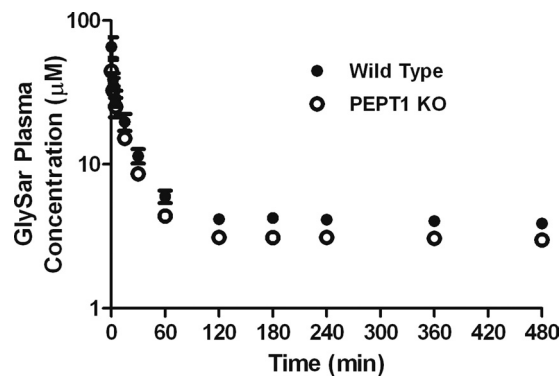


FIG. 4. Plasma concentrations of GlySar as a function of time over 480 min in wild-type and KO mice after an intravenous bolus dose of 10 nmol/g. Data are expressed as mean \pm S.E. ($n = 4-8$).

profile of GlySar was very different between the two genotypes and the absorption rate was slower in *Pept1* knockout mice; 3) the oral absorption GlySar was linear over 1 to 100 nmol/g doses, but it was reduced to a minor extent (<20 and 35% , respectively) at 1000 and 5000 nmol/g doses (this change was observed in both genotypes); and 4) with the exception of intestines, changes in tissue distribution were unremarkable between wild-type and *Pept1* knockout mice, largely reflecting differences in systemic exposure of the dipeptide. This study demonstrates that, under in vivo conditions, PEPT1 maintains a very high capacity for absorbing GlySar and potentially other peptide/mimetic substrates.

GlySar was studied over a 1 to 5000 nmol/g dose range because it reflects the physiological range of daily protein consumption. According to Ganapathy et al. (2006), it was estimated that di/tripeptides in the intestinal lumen can reach concentrations as high as 100 mM after

the digestion of protein. Given mouse body weights of 20 g and assuming a gastric volume of 0.4 ml (McConnell et al., 2008) plus 0.2 ml for the gavage volume, gastrointestinal concentrations of GlySar would approximately be 0.033, 0.33, 3.3, 33, and 167 mM, respectively, at oral doses of 1, 10, 100, 1000, and 5000 nmol/g dipeptide. The significance of these concentrations depends upon several factors, including its relation to the K_m of GlySar, which has been reported according to bulk ($K_m = 20$ mM) and intestinal wall ($K_m = 6$ mM) concentration values using an in situ intestinal perfusion model (Jappap et al., 2010).

Intestinal absorption is influenced by many factors, including intrinsic drug permeability, pore radius of the paracellular pathway, thickness of the mucous layer, membrane surface area, regional membrane fluidity, luminal drug concentration, and gastrointestinal residence time. Among these factors, permeability through the membrane, luminal drug concentration, and residence time are considered to be the most important factors for oral drug absorption (Kimura and Higaki, 2002; Masaoka et al., 2006). Luminal drug concentrations may change after oral administration because of intestinal absorption and by changes in fluid volume in each intestinal segment. In wild-type mice, the concentration of GlySar probably decreases rapidly and continuously as the dipeptide travels down the intestinal tract because of abundant PEPT1 expression in duodenal, jejunal, and ileal segments of small intestine (Jappap et al., 2010). As a result, one may not observe a dramatic limitation in GlySar absorption because, even at higher oral doses, intestinal concentrations of GlySar exceeding its K_m value might not be attained to saturate PEPT1. On the other hand, *Pept1* knockout mice, because of the lack of PEPT1-mediated GlySar absorption, probably have higher concentrations of dipeptide available in late segments of small intestine. As a result, the higher driving force for passive permeability in these regions, compared with wild-type

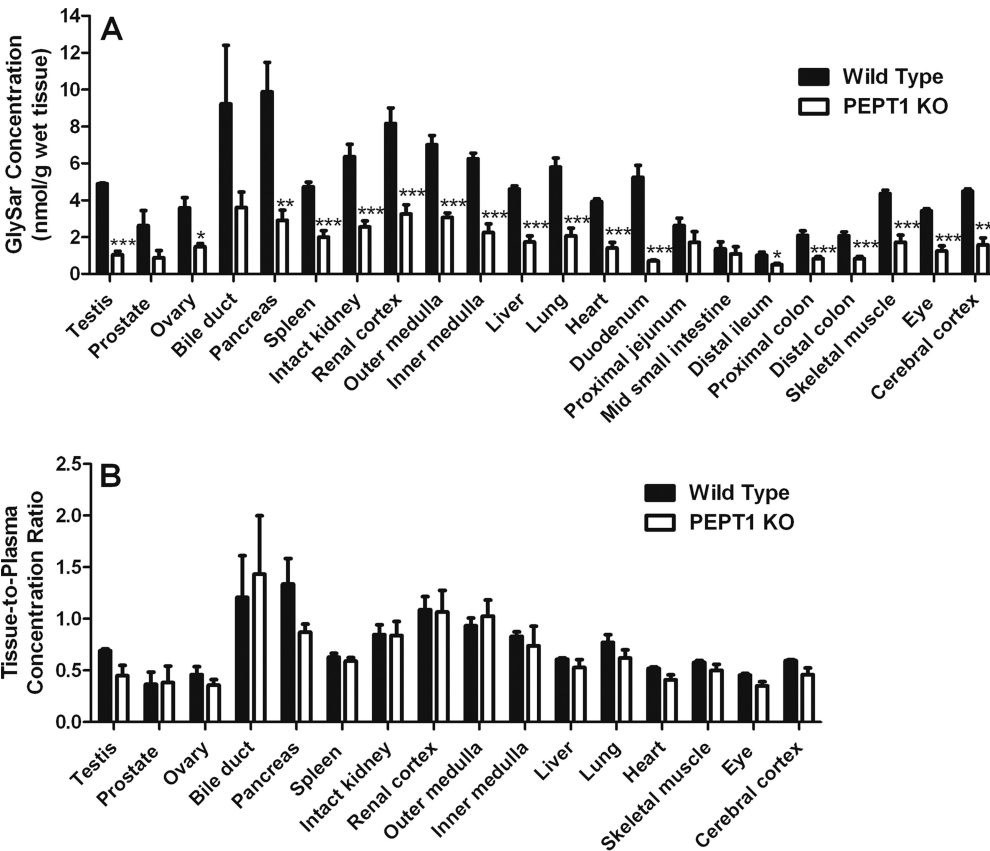


FIG. 5. Tissue concentrations (A) and tissue-to-plasma concentration ratios (B) of GlySar in wild-type and KO mice 1 h after an oral gavage of 10 nmol/g. Data are expressed as mean \pm S.E. ($n = 6$). *, $p < 0.05$; **, $p < 0.01$; and ***, $p < 0.001$ compared with wild-type mice.

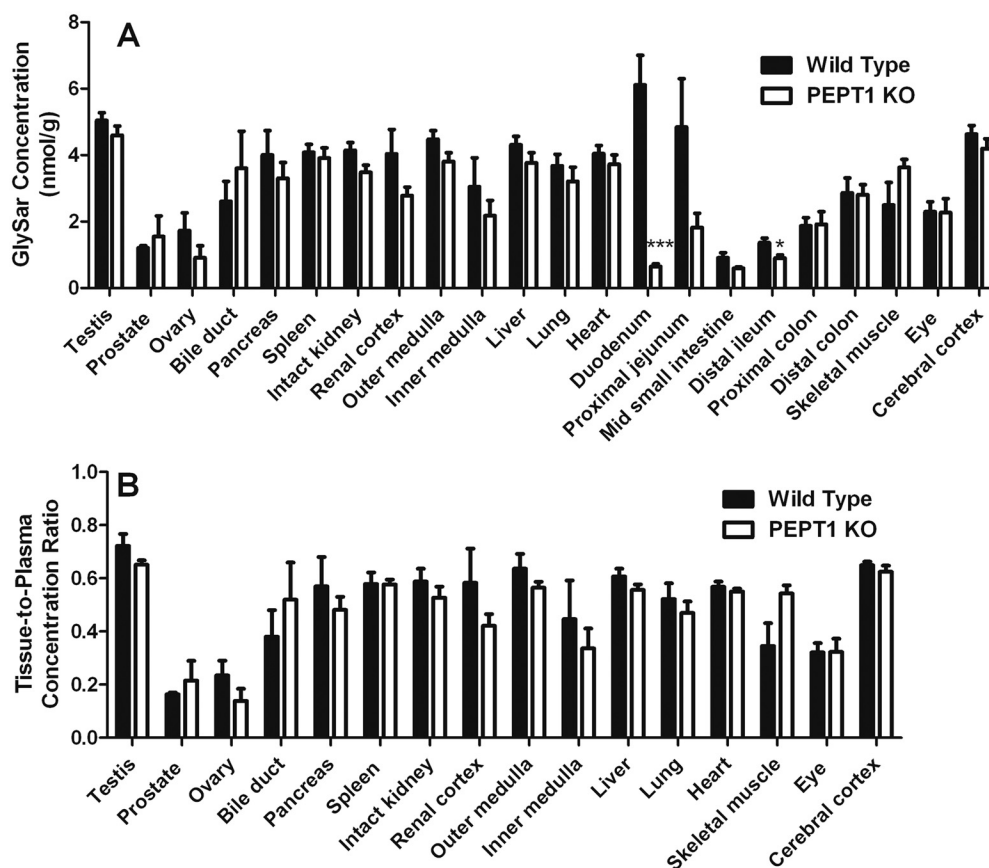


FIG. 6. Tissue concentrations (A) and tissue-to-plasma concentration ratios (B) of GlySar in wild-type and KO mice 8 h after an oral gavage of 10 nmol/g. Data are expressed as mean \pm S.E. ($n = 6$). *, $p < 0.05$; **, $p < 0.01$; and ***, $p < 0.001$ compared with wild-type mice.

animals, might explain the second rise in plasma concentrations of GlySar in *Pept1* knockout mice (i.e., from 120 to 240 min; Fig. 1). Still, it is unclear why a second rise in GlySar was not observed by Hu et al. (2008) after a 5 nmol/g oral dose of dipeptide. Notwithstanding this uncertainty, erratic absorption profiles have also been explained by the presence of enterohepatic circulation (Roberts et al., 2002), fractionated gastric emptying (Oberle and Amidon, 1987), absorption windows along the intestinal tract (Gramatté et al., 1994), and a presystemic storage compartment (Weitschies et al., 2005). Using a previously described high-performance liquid chromatography method with radiochemical detection (Ocheltree et al., 2005), GlySar instability was discounted as a possible confounding factor because, after oral dosing, no differences were observed between the two genotypes after 8- ($\geq 80\%$ unchanged) and 24-h urinary collections (77% unchanged).

As noted before, the dose-corrected AUC values of GlySar were 20% lower at the 1000 versus 1 nmol/g oral dose and 35% lower at the 5000 versus 1 nmol/g oral dose (Fig. 3). Although this finding suggests that intestinal PEPT1 may become saturated at the two higher doses, precipitation of GlySar in the gastrointestinal tract is also possible. In fact, a 10,000 nmol/g oral dose was omitted from our initial study design because of GlySar precipitating out of the aqueous solution. Masaoka et al. (2006) reported that, for poorly soluble compounds, concentrations in the small intestine could be 2- to 5-fold greater than anticipated because of rapid water absorption in the jejunum. Moreover, it is very unlikely that PEPT1 saturation alone was responsible for the reduction in dose-corrected AUC values because similar results were found in *Pept1* knockout mice. Taken as a whole, it is difficult to distinguish which mechanism is operative in wild-type mice and may, in fact, reflect saturation of intestinal PEPT1 and precipitation of GlySar. In *Pept1* knockout mice, reduced AUC

values relative to oral dose are probably due to precipitation of dipeptide in the small intestine.

During previous in situ single-pass perfusions, the jejunal permeability of GlySar was reduced by $>90\%$ in *Pept1* knockout compared with wild-type mice (Jappari et al., 2010). Although the present in vivo study corroborates the relevance of intestinal PEPT1 in oral dipeptide absorption, the magnitude of change was smaller than expected. Given that GlySar is transported by PEPT1 and that PEPT1 is abundantly expressed in all regions of mouse small intestine, its systemic exposure in *Pept1* knockout mice was 40, 55, and 70% of that in wild-type mice over 2, 4, and 8 h, respectively, and not 10-fold different. Thus, it is obvious that in situ intestinal perfusions, although mechanistically valid, do not necessarily reflect expected outcomes under physiological in vivo conditions in which luminal drug concentrations and gastrointestinal residence times are operative. Other mechanisms (e.g., passive permeability and paracellular permeability), as suggested by Chen et al. (2010) using everted jejunal sacs, may play a bigger role in the in vivo absorption of GlySar than previously believed, especially in the absence of PEPT1. GlySar is sufficiently small (mol. wt. 146) such that it may take advantage of the small intestine's residual length and passive permeability potential. By maintaining sufficient contact with epithelial cells of the duodenum, jejunum, and ileum, the passive absorption of GlySar may be increased in *Pept1* knockout mice, thereby diminishing the "apparent" role of intestinal PEPT1 in drug absorption. Although speculative, this reasoning is in agreement with the findings of Hironaka et al. (2009), who reported that PEPT1 contributed to one-half of the total absorption of cephalexin. These authors also noted that, during simulation studies, an 83% bioavailability would be expected for cephalexin in the absence of PEPT1 function because of a compensatory passive diffusion. It should be appreciated that other POT family members

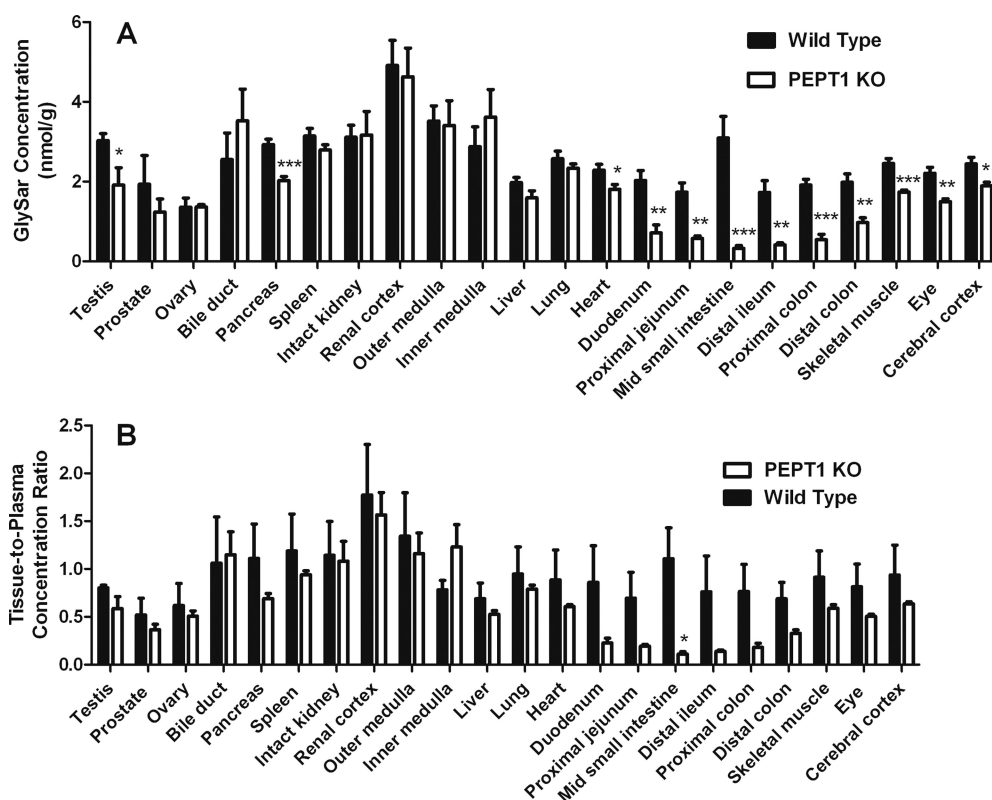


FIG. 7. Tissue concentrations (A) and tissue-to-plasma concentration ratios (B) of GlySar in wild-type and KO mice 8 h after an intravenous bolus dose of 10 nmol/g. Data are expressed as mean \pm S.E. ($n = 6$). *, $p < 0.05$; **, $p < 0.01$; and ***, $p < 0.001$ compared with wild-type mice.

(i.e., PEPT2, PHT1, and PHT2) were not upregulated during PEPT1 ablation (Hu et al., 2008) and therefore cannot explain the greater than expected absorption/systemic exposure of GlySar in *Pept1* knockout mice.

Studies comparing the pharmacokinetics of GlySar in wild-type and *Pept2* null mice have indicated that, of the 46% of dipeptide reabsorbed in the kidney of wild-type mice, PEPT2 and PEPT1 accounted for 86 and 14%, respectively, of this process (Ocheltree et al., 2005). Because GlySar is metabolically stable, one would expect the AUC of dipeptide to be 14% lower in *Pept1* knockout than wild-type mice when administered intravenously to both genotypes. Although the plasma concentration-time profiles of GlySar were almost superimposable between wild-type and *Pept1* null animals in the one study (Hu et al., 2008), the systemic exposure of intravenously administered GlySar in the present study was 24% lower in *Pept1* knockout mice than wild-type animals. Given that both studies were not designed in a crossover fashion, and there is variability between animals and experimental time periods, a 12% difference (on average) is reasonably close to the 14% difference that would be predicted from other experiments. Just as tissue distribution differences of GlySar, during PEPT2 ablation, are most noticeable in the kidney and choroid plexus (i.e., tissues that abundantly express this protein) (Ocheltree et al., 2005), the most noticeable differences in GlySar tissue distribution, during PEPT1 ablation (i.e., this study), are consistently found in the small intestine. However, once outside of the enteric system, PEPT1 has little if any influence on the tissue distribution of GlySar, especially when normalized for differences in dipeptide plasma concentration. Alternatively, one cannot exclude the possibility that biological variation may preclude minor differences from being observed in PEPT1-mediated effects on GlySar tissue distribution.

Mouse models of PEPT1 appear to be reasonable surrogates of its human ortholog for several reasons. First, the transport properties of peptides/mimetics are similar with respect to driving forces, substrate

specificity, and substrate affinity in cell culture systems expressing human and mouse PEPT1 (Liang et al., 1995; Mackenzie et al., 1996; Fei et al., 2000). Second, PEPT1 is found in the appropriate location of renal and intestinal tissues, with comparable expression levels in both species (Liang et al., 1995; Zhang et al., 2004; Hu et al., 2008). In particular, immunolocalization studies demonstrate that PEPT1 is expressed in the apical membrane of duodenum, jejunum, and ileum of human and mouse, with little or no expression in colon (Walker et al., 1998; Groneberg et al., 2001). Third, gene expression studies show that mouse and humans have intestinal expression levels of PEPT1 that are similar, whereas PEPT1 protein in rat is severalfold greater (Kim et al., 2007). Finally, mouse and human orthologs have high similarity in their genomic organization (Urtti et al., 2001).

In conclusion, our study is unique in providing the first comprehensive analysis of the absorption profile of a dipeptide after escalating oral doses. In particular, we demonstrated that the absorption rate of GlySar was dramatically altered by PEPT1 ablation. Although GlySar's extent of absorption was significantly reduced in *Pept1* knockout mice, it was less than predicted, probably reflecting the continuous passive diffusion of GlySar as it traveled down the entire length of small intestine. Other than small intestine, the effect of PEPT1 on GlySar tissue distribution was unremarkable. Future studies will be directed at studying the in vivo absorption and disposition of peptide-like drugs (e.g., cefadroxil and valacyclovir) and, in particular, to test whether intestinal PEPT1 is saturable at therapeutic doses of drug.

Acknowledgments

We thank Brendon Ladd, University of Michigan Department of Pharmacology, for his generous help in performing intravenous injections during the in vivo studies.

Authorship Contributions

Participated in research design: Jappara, Hu, and Smith.

Conducted experiments: Jappara.

Performed data analysis: Jappara.

Wrote or contributed to the writing of the manuscript: Jappara, Hu, and Smith.

References

- Bhardwaj RK, Herrera-Ruiz D, Eltouky N, Saad M, and Knipp GT (2006) The functional evaluation of human peptide/histidine transporter 1 (hPHT1) in transiently transfected COS-7 cells. *Eur J Pharm Sci* **27**:533–542.
- Bockman DE, Ganapathy V, Oblak TG, and Leibach FH (1997) Localization of peptide transporter in nuclei and lysosomes of the pancreas. *Int J Pancreatol* **22**:221–225.
- Brandsch M, Knütter I, and Bosse-Doenecke E (2008) Pharmaceutical and pharmacological importance of peptide transporters. *J Pharm Pharmacol* **60**:543–585.
- Chen M, Singh A, Xiao F, Dringenberg U, Wang J, Engelhardt R, Yeruva S, Rubio-Aliaga I, Nässli AM, Kottra G, et al. (2010) Gene ablation for PEPT1 in mice abolishes the effects of dipeptides on small intestinal fluid absorption, short-circuit current, and intracellular pH. *Am J Physiol Gastrointest Liver Physiol* **299**:G265–G274.
- Daniel H and Kottra G (2004) The proton oligopeptide cotransporter family SLC15 in physiology and pharmacology. *Pflugers Arch* **447**:610–618.
- Fei YJ, Kanai Y, Nussberger S, Ganapathy V, Leibach FH, Romero MF, Singh SK, Boron WF, and Hediger MA (1994) Expression cloning of a mammalian proton-coupled oligopeptide transporter. *Nature* **368**:563–566.
- Fei YJ, Sugawara M, Liu JC, Li HW, Ganapathy V, Ganapathy ME, and Leibach FH (2000) cDNA structure, genomic organization, and promoter analysis of the mouse intestinal peptide transporter PEPT1. *Biochim Biophys Acta* **1492**:145–154.
- Ganapathy V, Gupta N, and Martindale RG (2006) *Protein Digestion and Absorption, in Physiology of the Gastrointestinal Tract*, 4th ed (Johnson LR ed), pp 1667–1692, Elsevier, Burlington.
- Gramatté T, el Desoky E, and Klotz U (1994) Site-dependent small intestinal absorption of ranitidine. *Eur J Clin Pharmacol* **46**:253–259.
- Groneberg DA, Döring F, Eynott PR, Fischer A, and Daniel H (2001) Intestinal peptide transport: ex vivo uptake studies and localization of peptide carrier PEPT1. *Am J Physiol Gastrointest Liver Physiol* **281**:G697–G704.
- Herrera-Ruiz D and Knipp GT (2003) Current perspectives on established and putative mammalian oligopeptide transporters. *J Pharm Sci* **92**:691–714.
- Herrera-Ruiz D, Wang Q, Gudmundsson OS, Cook TJ, Smith RL, Faria TN, and Knipp GT (2001) Spatial expression patterns of peptide transporters in the human and rat gastrointestinal tracts, Caco-2 in vitro cell culture model, and multiple human tissues *AAPS PharmSci* **3**:E9.
- Hironaka T, Itokawa S, Ogawara K, Higaki K, and Kimura T (2009) Quantitative evaluation of PEPT1 contribution to oral absorption of cephalexin in rats. *Pharm Res* **26**:40–50.
- Hu Y, Smith DE, Ma K, Jappara D, Thomas W, and Hillgren KM (2008) Targeted disruption of peptide transporter Pept1 gene in mice significantly reduces dipeptide absorption in intestine. *Mol Pharm* **5**:1122–1130.
- Jappara D, Wu SP, Hu Y, and Smith DE (2010) Significance and regional dependency of peptide transporter (PEPT) 1 in the intestinal permeability of glycylsarcosine: in situ single-pass perfusion studies in wild-type and Pept1 knockout mice. *Drug Metab Dispos* **38**:1740–1746.
- Kim HR, Park SW, Cho HJ, Chae KA, Sung JM, Kim JS, Landowski CP, Sun D, Abd El-Aty AM, Amidon GL, et al. (2007) Comparative gene expression profiles of intestinal transporters in mice, rats and humans. *Pharm Res* **56**:224–236.
- Kimura T and Higaki K (2002) Gastrointestinal transit and drug absorption. *Biol Pharm Bull* **25**:149–164.
- Knütter I, Rubio-Aliaga I, Boll M, Hause G, Daniel H, Neubert K, and Brandsch M (2002) H⁺-peptide cotransport in the human bile duct epithelium cell line SK-ChA-1. *Am J Physiol Gastrointest Liver Physiol* **283**:G222–G229.
- Liang R, Fei YJ, Prasad PD, Ramamoorthy S, Han H, Yang-Feng TL, Hediger MA, Ganapathy V, and Leibach FH (1995) Human intestinal H⁺/peptide cotransporter: Cloning, functional expression, and chromosomal localization. *J Biol Chem* **270**:6456–6463.
- Lu H and Klaassen C (2006) Tissue distribution and thyroid hormone regulation of Pept1 and Pept2 mRNA in rodents. *Peptides* **27**:850–857.
- Ma K, Hu Y, and Smith DE (2011) Peptide transporter 1 is responsible for intestinal uptake of the dipeptide glycylsarcosine: studies in everted jejunal rings from wild-type and Pept1 null mice. *J Pharm Sci* **100**:767–774.
- Mackenzie B, Loo DD, Fei Y, Liu WJ, Ganapathy V, Leibach FH, and Wright EM (1996) Mechanisms of the human intestinal H⁺-coupled oligopeptide transporter hPEPT1. *J Biol Chem* **271**:5430–5437.
- Masaoka Y, Tanaka Y, Kataoka M, Sakuma S, and Yamashita S (2006) Site of drug absorption after oral administration: assessment of membrane permeability and luminal concentration of drugs in each segment of gastrointestinal tract. *Eur J Pharm Sci* **29**:240–250.
- McConnell EL, Basit AW, and Murdan S (2008) Measurements of rat and mouse gastrointestinal pH, fluid and lymphoid tissue, and implications for in-vivo experiments. *J Pharm Pharmacol* **60**:63–70.
- Oberle RL and Amidon GL (1987) The influence of variable gastric emptying and intestinal transit rates on the plasma level curve of cimetidine; an explanation for the double peak phenomenon. *J Pharmacokinet Biopharm* **15**:529–544.
- Ocheltree SM, Shen H, Hu Y, Keep RF, and Smith DE (2005) Role and relevance of peptide transporter 2 (PEPT2) in the kidney and choroid plexus: in vivo studies with glycylsarcosine in wild-type and PEPT2 knockout mice. *J Pharmacol Exp Ther* **315**:240–247.
- Roberts MS, Magnusson BM, Burczynski FJ, and Weiss M (2002) Enterohepatic circulation: physiological, pharmacokinetic and clinical implications. *Clin Pharmacokinet* **41**:751–790.
- Rubio-Aliaga I and Daniel H (2008) Peptide transporters and their roles in physiological processes and drug disposition. *Xenobiotica* **38**:1022–1042.
- Rühl A, Hoppe S, Frey I, Daniel H, and Schemann M (2005) Functional expression of the peptide transporter PEPT2 in the mammalian enteric nervous system. *J Comp Neurol* **490**:1–11.
- Saito H, Okuda M, Terada T, Sasaki S, and Inui K (1995) Cloning and characterization of a rat H⁺/peptide cotransporter mediating absorption of beta-lactam antibiotics in the intestine and kidney. *J Pharmacol Exp Ther* **275**:1631–1637.
- Shen H, Ocheltree SM, Hu Y, Keep RF, and Smith DE (2007) Impact of genetic knockout of PEPT2 on cefadroxil pharmacokinetics, renal tubular reabsorption, and brain penetration in mice. *Drug Metab Dispos* **35**:1209–1216.
- Shen H, Smith DE, Yang T, Huang YG, Schnermann JB, and Brosius FC 3rd (1999) Localization of PEPT1 and PEPT2 proton-coupled oligopeptide transporter mRNA and protein in rat kidney. *Am J Physiol* **276**:F658–F665.
- Thamotharan M, Lombardo YB, Bawani SZ, and Adibi SA (1997) An active mechanism for completion of the final stage of protein degradation in the liver, lysosomal transport of dipeptides. *J Biol Chem* **272**:11786–11790.
- Urtti A, Johns SJ, and Sadée W (2001) Genomic structure of proton-coupled oligopeptide transporter hPEPT1 and pH-sensing regulatory splice variant. *AAPS PharmSci* **3**:E6.
- Walker D, Thwaites DT, Simmons NL, Gilbert HJ, and Hirst BH (1998) Substrate upregulation of the human small intestinal peptide transporter, hPepT1. *J Physiol* **507** (Pt 3):697–706.
- Weitschies W, Bernsdorf A, Giessmann T, Zschiesche M, Modess C, Hartmann V, Mrazek C, Wegner D, Nagel S, and Siegmund W (2005) The talinolol double-peak phenomenon is likely caused by presystemic processing after uptake from gut lumen. *Pharm Res* **22**:728–735.
- Zhang EY, Emerick RM, Pak YA, Wrighton SA, and Hillgren KM (2004) Comparison of human and monkey peptide transporters: PEPT1 and PEPT2. *Mol Pharm* **1**:201–210.
- Zhou X, Thamotharan M, Gangopadhyay A, Serdikoff C, and Adibi SA (2000) Characterization of an oligopeptide transporter in renal lysosomes. *Biochim Biophys Acta* **1466**:372–378.

Address correspondence to: Dr. David E. Smith, Department of Pharmaceutical Sciences, University of Michigan, 4742C Medical Sciences II, 1150 W. Medical Center Drive, Ann Arbor, MI 48109-5633. E-mail: smithb@umich.edu
